J. of the Chosun Natural Science
Vol. 4, No. 1 (2011) pp. 1 – 6

Review Article

Chemical and Physical Properties of Porous Silicon

Seunghyun Jang†

Abstract

The properties of porous silicon, such as substrate properties, porosity, thickness, refractive index, surface area, and optical properties of porous silicon were reviewed. Some properties, such as porosity, refractive index, thickness, pore diameter, multi-structures, and optical properties, are strongly dependent on the anodization process parameters. These parameters include HF concentration, current density, anodization time, and silicon wafer type and resistivity.

Key words : Porous Silicon, Optical Property, Refractive Index, Porosity

1. Introduction

Porous silicon (PSi) material, an electrochemical product of silicon, is a natural nano-structured material that can be prepared easily without much sophistication. PSi was discovered by Ulhir[1] at Bell Labs, USA in 1956, followed by Turner[2] during a study on the electropolishing of silicon wafer in hydrofluoric acid solution. In the 1970's, it was reported that the silicon of PSi in the porous structure could be easily transformed into silicon dioxide by thermal oxidation, and used as a dielectric material[3-6].

In 1990, L. T. Canham first reported that PSi is efficient, tunable, room temperature luminescent materials in the visible range[7]. Afterward, the interest in the field of porous silicon grew exponentially. From this point on, a large number of academic and industrial researchers from all over the world began to study the pore structure of PSi[8,9], light emission mechanism and properties[10,11], surface modification chemistry[12,13], and feasibility for optoelectronic and other possible applications[14,15].

The many favorable characteristics and the great interest in PSi have given rise to a variety of new applications such as light emitting devices[15], multi-layer structure for photonic crystals[16], energy conversion for solar cell [17], chemical and biological sensors[18-23], drug delivery system[24], ultrasound generators[25], micro-engineering[26], astrophysics[27], signal processing[28], and nuclear science[29]. Due to these multi-functional applications of PSi, recently it has been proposed to be an educational vehicle for introducing nano-technology and inter-disciplinary materials science by eminent scientists in the field[30].

In this paper, the properties of PSi, such as substrate properties, porosity, thickness, refractive index, surface area, and optical properties of PSi were reviewed and reported.

2. Experimental Section

2.1. Preparation of PSi

The anodization cell is made of Teflon, which is resistive against attack from the hydrofluoric acid electrolyte. The aluminum foil serves as the anode and it is sandwiched between the top and bottom parts of the Teflon cell. For a better contact, a platinum wire is placed against the silicon wafer where leads can be connected. The cathode is a circular platinum wire that is submerged in the hydrofluoric acid electrolyte. The cathode is held in place, three wing nuts hold the entire anodization cell together during the electrochemical etching process. The hydrofluoric acid electrolyte is placed inside the top part of the Teflon cell. Enough electrolyte must be present to supply the required fluorine ions and to cover the platinum wire cathode. The top part of the Teflon cell has a circular window of area 1.2 cm^2 which exposes the silicon to hydrofluoric acid and forms the PSi. The entire electrochemical process

Department of Chemistry, University of Wisconsin, Madison, 1101 University Ave., Madison, WI 53706 (USA)

†Corresponding author: shjang@chem.wisc.edu
(Received : March 2, 2011, Revised : March 16, 2011, Accepted : March 21, 2011)

is carried out under constant current supplied by a computer controlled Keithley 2420 power sourcemeter.

2.2. Instrumentation and Data Acquisition

Optical reflectivity spectra are measured using a tungsten halogen lamp and an Ocean Optics S2000 CCD spectrometer fitted with a fiber optic input. The reflected light collection end of the fiber optic is positioned at the focal plane of the optical microscope.

3. Result and Discussion

Some properties, such as porosity, refractive index, thickness, pore diameter, multi-structures, and optical properties, are strongly dependent on the anodization process parameters. These parameters include HF concentration, current density, anodization time, and silicon wafer type and resistivity.

3.1. Substrate Properties

Silicon substrates are identified by properties such as dopant type (i.e., n-type or p-type), substrate resistivity, dopant concentration, and substrate orientation. During anodization, dopant of the silicon substrate plays a significant role. Since holes (h^+) are the most important element in the chemical reaction leading to the formation of PSi, the use of p-type wafer is the most popular. However, n-type wafer can be used with external illumination.

Substrate resistivity determines the achievable thickness of PSi. For example, a very low resistivity wafer (<0.01 Ω-cm) is capable of producing thicker PSi compared to a wafer with a higher resistivity (>10 Ω-cm) under same anodization conditions.

The morphology of the PSi can be grouped into four categories based on doping concentration: p, p^+, p^{++}, n, n^+, and n^{++} [31]. For p-type silicon wafer, the pore diameters and interpore spacing are very small (20-100 Å). As the dopant concentration increases, the pore diameter and spacing increase slightly (100-1000 Å). For n-type silicon, the pore diameters are considerably larger than those of the p-type substrate.

Substrate orientation is also important in the structure of the PSi morphology. The main pore growth direction is essntially the same irrespective of the substrate orientation, dopant concentration or anodization conditions[32-33].

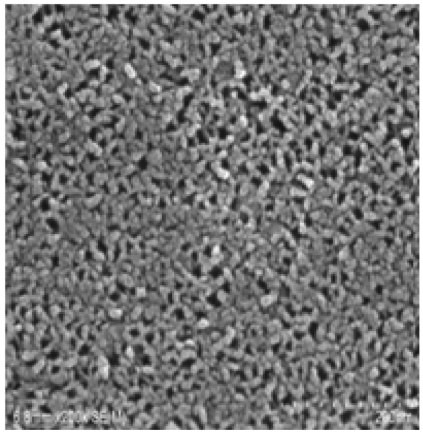

Fig. 1. Surface morphology of porous silicon.

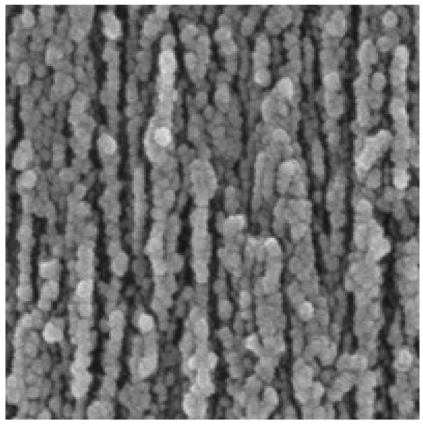

Fig. 2. Cross sectional morphology of porous silicon.

The pore shape, pore size, and orentation of porous siliconlayers depend on the surface orentation and doping level and type, temperature, the current density, and the composition of the etching solution. For mono-layered PSi, an anodic etch of p-type silicon wafer with resistivities of 0.1~10 Ω·cm in ethanolic HF solution generally produced PSi single layer with a network of micropores, rather than meso- or macropores. The shape, size, and orientation of pores of PSi layers depended on surface orientation and the dopant level of the crystalline silicon substrate as well as the applied current density, the temperature, and the concentration of the HF etching solution. The pore size of p-type PSi can be increased by increasing the concentration of the dopant and decreasing the aqueous HF concentration. High current densities resulted in the desired well-defined cylindrical macropores, rather than the random

orientation of highly interconnected micropores.

The surface morphology of PSi was obtained with cold field emission scanning electron microscope (FE-SEM) and shown in Fig. 1. The surface image of PSi indicated that the distributions of pores were even.

The cross sectional morphology of PSi was obtained with with cold FE-SEM and shown in Fig. 2. FE-SEM image of PSi indicated that the prepared PSi had cylindrical mesopores and a depth of a few microns.

3.2. Porosity

The most important quantity when characterizing a porous materials is the porosity which is defined as the ratio of the empty pore volume to the total volume. The porosity of a PSi can be calculated gravimetrically using following equation[34]:

$$\text{Porosity } (\%) = \frac{m_1 - m_2}{m_1 - m_3}$$

Where m_1 is the mass of the initial silicon wafer in grams, m_2 is the mass of the silicon wafer after anodization in grams, m_3 is the mass of the silicon wafer after dissolution of the porous layer in grams. The dissolution of PSi is performed using a 0.1 M aqueous solution of sodium hydroxide (NaOH).

This gravimetric method is applicable in cases where the PSi layer is sufficiently thick (> 5 μm). The differnce in masses is larger than the amount of error induced in the measurements. However, when the PSi layer is thin (< 200 nm), the mass difference is the same order of magnitude as the error in measurements, and the porosity value obtained is unreliable.

3.3. Thickness

The thickness of PSi can be determined using either non-destructive or destructive techniques. One non-destructive technique is the use of an ellipsometer which requires the extensive understanding of the refractive index. For the PSi samples, the index is difficult to determine since the porosity varies vertically with depth. There are two available destructive techniques that can be used with significant ease. One determines the approximate PSi thickness using following equation:

$$\text{Thickness} = \frac{M_1 - M_3}{S \cdot d}$$

Where M_1 is the mass of the original silicon wafer, M_3 is the wafer with anodized material removed, S is the area of the PSi sample, and d is the density of the silicon substrate.

The second and more accurate technique uses a field emission scanning electron microscope (FE-SEM) after scribing the PSi sample to visualize a cross sectional view. This technique can resolve the thickness of PSi to a few nanometers as well as provide additional information on the PSi morphology.

3.4. Refractive Index

The refractive index is one of the important property of PSi. This property controls the reflection and transmission of waves incident on the PSi-air interface. There are many approximations that predict the refractive index of PSi based on porosity[35-36]. However, none of them covers the entire porosity range with the same degree of high accuracy.

The refractive index of PSi is calculated by using the Bruggeman approximation as described below:

$$(1\text{-}P)\frac{\varepsilon_{Silicon} + \varepsilon_{porous\ silicon}}{\varepsilon_{Silicon} + 2\varepsilon_{porous\ silicon}} + (P)\frac{\varepsilon_{air} + \varepsilon_{porous\ silicon}}{\varepsilon_{air} + 2\varepsilon_{porous\ silicon}} = 0$$

where P is the porosity of porous silicon, $\varepsilon_{silicon}$ is the dielectric constant of silicon, ε_{air} is the dielectric constant of air, and $\varepsilon_{porous\ silicon}$ is the dielectric constant of porous silicon.

3.4. Surface Area

PSi has a very large surface area (1-500 m^2/cm^3) defined as the accessible area of solid surface per unit of material. This characteristic gives PSi the ability to act as a host to many inorganic and organic materials, resulting in many potential applications. A standard method used to measure the specific surface area is the BET (Brunauer-Emmett-Teller) method[37]. This method is based on the adsorption of gases by the porous structure.

3.5. Optical Properties

The optical properties of PSi are discussed in a wide spectral range from the infrared to the ultraviolet. PSi has two optical properties such as photoluminescence (PL) for n-type with external illumination (300 W tungsten lamp) and optical reflectivity (Fabry-Perot fringe) for p-type as shown in Fig. 1. The ability of PSi to emit

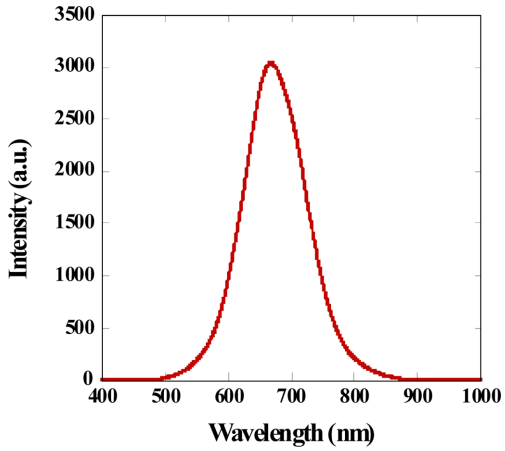

Fig. 3. Photoluminescence spectrum of porous silicon.

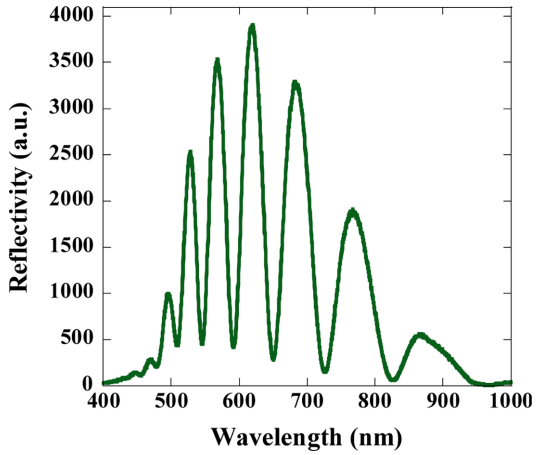

Fig. 4. Reflectivity spectrum of porous silicon.

and reflect in visible range is the most attractive property of the material. One explanation for the visible luminescence is based on the nanometer-size crystalline structure for PSi[38-40].

PL spectrum of PSi shown in Figure 3 has been obtained with Ocean Optics LS-1 (blue LED). Typical photoluminescence wavelength appeared as strong red emission whose wavelengths range between 500 and 800 nm. The wavelength of the photoluminescence maximum of porous silicon can be readily tuned by adjusting the preparation conditions such as etching times and the concentration of etching solution. An important feature of this material is that its photoluminescence properties can be controlled by interfacial electron-, hole-, and energy-transfer processes. For example, many organic aromatic molecules have been shown to efficiently quench photoluminescence from porous silicon. Comparison of the quenching data with the oxidation potentials, reduction potentials, and triplet energy levels led to the conclusion that the quenching process for aromatic molecules is predominantly driven by energy transfer.

Optical reflectivity spectrum of PSi showing Febry-Perot fringe pattern has been measured by using tungsten-halogen lamp and an Ocean Optics S2000 charge-coupled detector (CCD) spectrometer fitted with a fiber optic input. The reflected light collection end of the fiber optic is positioned at the focal plane of the optical microscope as described in Fig. 4.

The interference or fringe patterns could be obtained from porous silicon layers anodized at different current densities. Fabry-Perot fringes using visible light illumination are observed on samples prepared at current densities between 150 and 600 mA/cm^2. Anodization of p-type silicon at a current density of 600 mA/cm^2 results in an obvious matte surface with a barely discernible fringe pattern, due to the increased light scattering occurring at the surface of the upper porous silicon layer. Electropolishing occurs at a current density higher than 700 mA/cm^2. The number of fringes in the observed wavelength range depends on the porosity as well as the thickness of the porous layer. Samples with thicknesses of approximately 3000 nm typically display 9-12 fringes in the 500-1000 nm wavelength region depending on the effective refractive index. The higher the current density, the fewer fringes are observed, consistent with the observation that higher current densities lead to samples with greater porosities.

3.6. Characterization of Porous Silicon

Diffuse reflectance FT-IR spectroscopy was used to monitor the oxidation and functionalization reactions of the porous silicon support. The FT-IR spectrum of the porous silicon layer immediately after anodization of the silicon wafer displays a characteristic broad band centered at 2118 cm^{-1} (Fig. 5) (overlap of the νSi-H_2 and νH-Si-O stretching vibrations). The νSi-H and νSi-H_3 stretching bands are not visible since backbone oxidation of the Si-Si bonds took place immediately after etching. Oxidation of the porous silicon layer with ozone results in the appearance of the characteristic large and broad Si-O-Si vibrational band around 1110

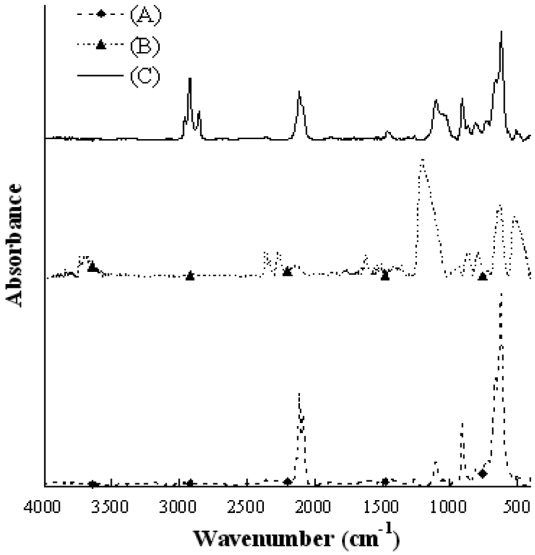

Fig. 5. FT-IR spectra of porous silicon.

cm^{-1} in the FT-IR spectrum. As expected, ozonolysis also leads to complete disappearance of the Si-H vibrational bands. A small band at 887 cm^{-1} assigned to δSi-OH is also observed. Exposure to ozone for longer periods led to complete disappearance of the Si-OH band because the formation of the Si-O-Si bonds is thermodynamically preferred.

4. Conclusion

The properties of porous silicon, such as substrate properties, porosity, thickness, refractive index, surface area, and optical properties of porous silicon are strongly dependent on the anodization process parameters. These parameters include HF concentration, current density, anodization time, and silicon wafer type and resistivity.

References

[1] A. Uhlir, "Electrolytic shaping of germanium and silicon", Bell Synt. Tech. J., Vol. 35, p. 333, 1956.
[2] D. R. Turner, "Electropolishing Silicon in Hydrofluoric Acid Solutions", J. Electrochem. Soc., Vol. 105, p. 402 1958.
[3] Y. Arita, K. Kato, and T. Sudo, "The n+-IPOS scheme and its applications to IC's", IEEE T. Electron Dev., Vol. 24, p. 757, 1977.
[4] T. Unagami and K. Kato, "Study of the Injection Type IPOS Scheme", Jpn. J. Appl. Phys., Vol. 16, p. 1635, 1977.
[5] K. Imai, "A new dielectric isolation method using porous silicon", Solid State Electron, Vol. 24, p. 159, 1981.
[6] F. Otoi, K. Anzai, H. Kitabayashi, K. Uchiho, and Y. Mizokami, "Fabrication of high speed 1 micron FIPOS/CMOS", J. Electrochem. Soc., Vol. 131, p. C319, 1984.
[7] L. T. Canham, "Silicon quantum wire array fabrication by electrochemical and chemical dissolution of wafers", Appl. Phys. Lett., Vol. 57, p. 1046, 1990.
[8] A. G. Cullis and L. T. Canham, "Visible light emission due to quantum size effects in highly porous crystalline silicon", Nature, Vol. 353, p. 335, 1991.
[9] Z. Sui, P. P. Leong, I. P. Herman, G. S. Higashi, and H. Temkin, "Raman analysis of light?emitting porous silicon", Appl. Phys. Lett., Vol. 60, p. 2086, 1992.
[10] C. Delerue, G. Allan, and M. Lannoo, "Theoretical aspects of the luminescence of porous silicon", Phys. Rev. B, Vol. 48, p. 11024, 1993.
[11] F. Koch, V. Petrova-koch, T. Muschik, A. nikolov, and V. Gavrilenko, "Fast Photoluminescence from Porous Silicon", Mater. Res. Soc. Symp. Proc., Vol. 298, p. 319, 1993.
[12] E. J. Lee, T. W. Bitner, J. S. Ha, M. J. Shane, and M. J. Sailor, "Light-Induced Reactions of Porous and Single-Crystal Si Surfaces with Carboxylic Acids", J. Am. Chem. Soc., Vol. 118, p. 5375, 1996.
[13] J. M. Buriak and M. J. Allen, "Lewis Acid Mediated Functionalization of Porous Silicon with Substituted Alkenes and Alkynes", J. Am. Chem. Soc., Vol. 120, p. 1339, 1998.
[14] A. Richter, P. steiner, F. Kozlowski, and W. Lang, "Current induced light emission from a porous silicon device", IEEE Electron Device Lett., Vol. 12, p. 691, 1991.
[15] K. D. Hirschmann, L. Tsybeskov, S. P. Duttagupta, and P. M. Fauchet, "Silicon-based visible light-emitting devices integrated into microelectronic circuits", Nature, Vol. 384, p. 338, 1996.
[16] C. Mazzoleni and L. Pavesi, "Application to optical components of dielectric porous silicon multilayers", Appl. Phys. Lett., Vol. 67, p. 2983, 1995.
[17] G. Smestad, M. Kunst, and C. Vial, "Photovoltaic response in electrochemically prepared photoluminescent porous silicon", Sol. Energy Mater. Sol. Cells, Vol. 26, p. 277, 1992.
[18] J. M. Lauerhaas and M. J. Sailor, "Chemical Mod-

ification of the Photoluminescence Quenching of Porous Silicon", Science, Vol. 261, p. 1567, 1993.
[19] H. Sohn, S. Letant , M. J. Sailor, and C. Trogler, "Detection of Fluorophosphonate Chemical Warfare Agents by Catalytic Hydrolysis with a Porous Silicon Interferometer", J. Am. Chem. Soc., Vol. 122, p. 5399, 2000.
[20] S. Letant and M. J. Sailor, "Molecular Identification by Time-Resolved Interferometry in a Porous Silicon Film", Adv. Mater., Vol. 13, p. 355, 2001.
[21] S. Chan, S. R. Horner, P. M. Fauchet, and B. L. Miller, "Identification of Gram Negative Bacteria Using Nanoscale Silicon Microcavities", J. Am. Chem. Soc., Vol. 123, p. 11797, 2001.
[22] H. Sohn, R. M. Calhoun, M. J. Sailor, and W. C. Trogler, "Detection of TNT and Picric Acid on Surfaces and in Seawater by Using Photoluminescent Polysiloles", Angew. Chem. Int. Ed., Vol. 40, p. 2104, 2001.
[23] H. Sohn, M. J. Sailor, D. magde, and W. C. Trogler, "Detection of Nitroaromatic Explosives Based on Photoluminescent Polymers Containing Metalloles", J. Am. Chem. Soc., Vol. 125, p. 3821, 2003.
[24] X, Li, J. L. Coffer, Y. D. Chen, R. F. Pinizzotto, J. Newey, and L. T. Canham, "Transition Metal Complex-Doped Hydroxyapatite Layers on Porous Silicon", J. Am. Chem. Soc., Vol. 120, p. 11706, 1998.
[25] N. Koshida, T. Nakajima, M. Yoshiyama, K. Ueno, T. Nakagawa, and H. Shinoda, "Ultrasound emission from porous silicon - Efficient thermoacoustic function as a depleted nanocrystalline system", Mater. Res. Soc. Symp. Proc., Vol. 536, p. 105, 1999.
[26] T. E. Bell, P. T. J. Gennissen, D. Demunter, and M. Kuhl, "Porous silicon as a sacrificial material", J. Micromech. Microeng., Vol. 6, p. 361, 1996.
[27] V. G. Zubko, T. L. Smith, and A. N. Witt, "Detection of Extended Red Emission in the Diffuse Interstellar Medium", J. Astrophys., Vol. 498, p. 501, 1998.
[28] V. P. Parkhutik, E. Matveeva, R. Perez, J. Alamo, and D. Beltraan, "Mechanism of large oscillations of anodic potential during anodization of silicon in H3PO4/HF solutions", Mater. Sci. Engn. B, Vol. 69-70, p. 53, 2000.
[29] V. P. Bondarenko, Y. V. Bogatirev, J. P. Colinge, L. N. Dolgyi, A. M. Dorofeev, and V. A. Yakovtseva, "Total gamma dose characteristics of CMOS devices in SOI structures based on oxidized porous silicon", IEEE. Trans. Nucl. Sci., Vol. 44, p. 1719, 1997.
[30] V. P. Parkhutik and L. T. Canham, "Derivatized Porous Silicon Mirrors: Implantable Optical Components with Slow Resorbability", Phys. Stat. Sol. A, Vol. 182, p. 591, 2000.
[31] R. L. Smith and S. D. Collins, "Porous silicon formation mechanisms", J. Appl. Phys., Vol. 71, p. R1, 1992.
[32] M. Christopersen, J. Carstensen, and H. Foll, "Parameter Dependence of Pore Formation in Silicon within a Model of Local Current Bursts", Phys. Stat. Sol. A, Vol. 182, p. 601, 2000.
[33] S. F. Chuang, S. D. Collins, and R. L. Smith, "Preferential propagation of pores during the formation of porous silicon: A transmission electron microscopy study", Appl. Phys. Lett., Vol. 55, p. 675, 1989.
[34] D. Brumhead, L. T. Canham, D. M. Seekings, and P. J. Tufton, "Gravimetric analysis of pore nucleation and propagation in anodised silicon", Electrochi. Acta., Vol. 38, p. 191, 1993.
[35] D. J. Bergman, "The dielectric constant of a composite material?A problem in classical physics", Phys. Rep. C, Vol. 43, p. 377, 1978.
[36] H. Looyenga, "Dielectric constants of heterogeneous mixtures", Physica, Vol. 31, p. 401, 1965.
[37] S. Brunauer, P. H. Emmett, and E. Teller, "Adsorption of Gases in Multimolecular Layers", J. Am. Chem. Soc., Vol. 60, p. 309, 1938.
[38] S. Sawada, N. Hamada, and N. Ookubo, "Mechanisms of visible photoluminescence in porous silicon", Phys. Rev. B, Vol. 49, p. 5236, 1994.
[39] A. J. Read, R. J. Needs, K. J. Nash, L. T. Canham, P. D. J. Calcott, and A. Qteish, "First-principles calculations of the electronic properties of silicon quantum wires", Phys. Rev. Lett., Vol. 69, p. 1232, 1992.
[40] Y. Kanemitsu, H. Uto, Y. Masumoto, T. Futagi, and H. Mimura, "Microstructure and optical properties of free-standing porous silicon films: Size dependence of absorption spectra in Si nanometer-sized crystallites", Phys. Rev. B, Vol. 48, p. 2827, 1993.